Influence of boundary slip on the acoustical properties of microfibrous absorbents

Olga Umnova, David Tsiklauri and Rodolfo Venegas

University of Salford, Acoustics Research Centre, Newton Building, M5 4WT Salford, UK
o.umnova@salford.ac.uk

In the past decades a variety of new highly porous materials with unusually small pores have been manufactured. In aerogels, for instance, pores can be less than 20 nm in diameter. The conventional models have to be modified when applied to describe acoustical properties of those materials. The non-slip condition on a pore surface is no longer valid and needs to be replaced by the Knudsen boundary condition. In attempt to provide an insight into the behaviour of microfibrous materials, an analytical model has been developed, which accounts for the boundary slip in a medium consisting of rigid parallel fibres assuming different directions of sound propagation with respect to fibres. It has been shown that the presence of the boundary slip leads to a significant change in model predictions. For instance, in a material with fibre radius 120 nm and 95% porosity the sound speed decreases and attenuation increases by more than 20% compared to the values obtained assuming no boundary slip. The effect is stronger for smaller size fibres, lower porosity values and for sound propagating parallel to fibres. Numerical computations have been performed to simulate oscillatory flow around the cylindrical fibres assuming Knudsen boundary conditions and the results have been compared with the analytical model predictions

1   Introduction

Although the majority of porous materials used currently in noise control applications have pores larger than a micrometer, a substantial number of new materials are being created with considerably smaller pores. In aerogels, for instance, pores can be as small as 20nm in diameter. In activated carbon, a considerable amount of pores range between 50 nm and 1000 nm. It turns out that conventional models have to be used with caution when predicting acoustical properties of the materials with such small pores.

Until recently all microstructure based models assumed the validity of no slip boundary conditions on the pore or inclusion surfaces. Those conditions are violated though if sound propagates in a highly confined volume [1] with a linear dimension *a* comparable to the molecular mean free path l_{mean}. For air at normal conditions $l_{mean} \approx 60nm$ and it grows as gas pressure decreases. The importance of the boundary slip is determined by the value of the Knudsen number defined as the ratio of the molecular mean free path to the characteristic linear size *a*: $Kn = \dfrac{l_{mean}}{a}$.

For sound propagation in a porous material, the difference between slip and no-slip boundary conditions can become important when the molecular mean free path is comparable to the average pore or inclusion size. Strictly speaking, the continuum, i.e. based on the equations of fluid mechanics, approach to sound propagation in a confined space can only be used in a so called Knudsen regime when $Kn \leq 0.1$ and imposes lower limit on the pore or inclusion size: $a \geq 10 l_{mean} = 600nm$. However, there are numerous evidences based on the comparisons with both measurements [2] and molecular dynamics simulations [3] that continuum approach still provides a good approximation even at much higher values of Knudsen number. In [2] for instance good agreement between data and the theory for the rarefied gas flow through the cylindrical channels is shown for Knudsen number as high as one. Several recent publications have been looking into the boundary slip effect on sound propagation through microporous materials using microstructure based approach. The homogenisation theory has been extended to account to the wall slip in [4,5]. Papers [2,3] focus on the rigid porous materials where the non-slip boundary condition on the pore wall has been replaced by Knudsen

boundary conditions, relating the tangential velocity on the rigid surface to the stress component. In several publications the elasticity of the frame has been accounted for assuming either empirical dependence of the slip velocity on the pore wall on frequency [6] or Knudsen boundary conditions [7]. In [2] the influence of thermal slip on complex compressibility function has been investigated. In all these publications the pore geometry was restricted to straight cylindrical channels. However there are certain types of porous materials for which this assumption seems to be too crude. In aerogels, for instance, porosity can be higher than 0.9 [8] while the cylindrical pore approximation is only applicable for the values below 0.785. In this paper, the model is developed for the acoustical properties of fibrous materials allowing for both velocity and temperature boundary slip. This was done in attempt to reflect the geometry of real highly porous fibrous absorbents. The fibres are assumed to be cylindrical and arranged in a regular square lattice. This simplification allows analytical approach and is convenient for the investigation of different regimes of sound propagation. Two fibre orientations in respect to sound propagation direction are considered to demonstrate the dependence of the slip effects on the geometry. The paper is organised as follows. In Section 2 the problem of oscillatory flow around cylindrical fibres is solved analytically. The method is based on the "cell model" used in [9] which is generalised to allow for the boundary slip. The problem of the heat transfer from the fibre has been solved accounting for the thermal slip. The analytical expressions for complex density and complex compressibility functions are derived. Section 3 describes numerical solution of the problem using finite element method. Comparisons between analytical and numerical results are presented here. Main findings are summarised in Conclusion.

2   Analytical model for the acoustical properties of regular array of cylinders with nonzero boundary slip

2.1   Complex tortuosity – fibres perpendicular and parallel to sound propagation direction

A detailed analysis of the approach presented in this part of the paper, assuming however non-slip boundary conditions, can be found elsewhere [9]. Here the brief outline of the necessary equations and their solutions as well as the modifications of the boundary conditions is presented.

The motion of incompressible fluid (air) around an infinitely long cylindrical fibre of radius a under oscillatory with angular frequency ω constant amplitude pressure gradient along x-axis $\partial_x P e^{-i\omega t} \vec{e}_x$ (Figure 1) is governed by the following equations:

$$-i\omega\rho_0\vec{u} = -grad p / a + \eta\Delta\vec{u} / a^2 - \partial_x P\vec{e}_x ,$$
$$div\vec{u} = 0 \tag{1}$$
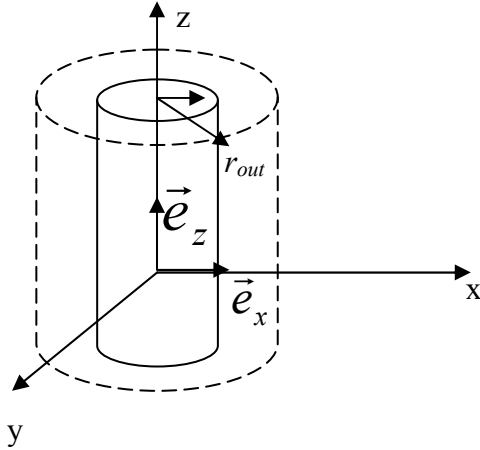
Figure1 Geometry of the problem

here $\vec{u}$ and p are particle velocity and pressure of the air. All spatial coordinates are normalised by the fibre radius a. Due to the symmetry, in cylindrical coordinates (r,θ,z), the particle velocity does not have a z-component and does not vary in z-direction.

Two boundary conditions are set on the fibre surface, i.e. condition of zero normal velocity component

$$u_r(r=1) = 0 \tag{2}$$

and Knudsen boundary condition for the tangential velocity component

$$u_\theta(r=1) = Kn\tau_{r\theta}(r=1)/\eta , \tag{3}$$

where $\tau_{r\theta} = \eta(\partial_\theta u_r / r + \partial_r u_\theta - u_\theta / r)$ is the component of the stress tensor.

In order to account for the influence of neighbouring fibres, each cylinder is assumed surrounded by an imaginary cell, whose radius is chosen so that the volume fraction of air in each cell is the same as the porosity ϕ of the whole array, i.e. $r_{out} = 1/\sqrt{1-\phi}$. Zero vorticity is assumed on that boundary

$$curl\vec{u}(r=r_{out}) = 0 \tag{4}$$

The total pressure drop over the boundary of the cell is equal to the macroscopic pressure gradient, i.e

$$p(r=r_{out}) = 0 . \tag{5}$$

Equations (1) with boundary conditions (2)-(5) fully determine the flow characteristics within the cell. Let's assume that $\vec{u} = \vec{v} + curl\vec{A}$, where $\vec{v} = v\vec{e}_x$, $v = \partial_x P/(i\omega\rho_0)$ and $\vec{A}$ is a vector potential. Due to the

symmetry, in cylindrical coordinates (r,θ,z) the vector potential has z-component $A_z = A(r)\sin\theta$ only and components of particle velocity are:

$$u_r = v\cos\theta + \partial_\theta A_z / r = (v + A(r)/r)\cos\theta$$
$$u_\theta = -v\sin\theta - \partial_r A_z = -(v + A'(r))\sin\theta . \tag{6}$$

Vorticity of $\vec{u}$ can now be calculated as

$$curl\vec{u} = (u_\theta / r + \partial_r u_\theta - \partial_\theta u_r / r)\vec{e}_z =$$
$$-(A'(r)/r + A''(r) - A(r)/r^2)\sin\theta\vec{e}_z = f(r)\sin\theta\vec{e}_z$$

where

$$f(r) = -(A'(r) + A(r)/r)' . \tag{7}$$

It can now be easily shown that pressure is equal to

$$p = \eta(\kappa^2 A'(r) - f'(r))r\cos\theta / a \tag{8}$$

where

$$\kappa = a\sqrt{i\omega\rho_0 / \eta} . \tag{9}$$

The absolute value of parameter κ is equal to the ratio of the fibre radius and the viscous boundary layer thickness $\delta_{visc} = \sqrt{2\eta / \omega\rho_0}$ ..

Equations (1) can be reduced now to a single equation for the function $f(r)$

$$f''(r) - f'(r)/r - f/r^2 + \kappa^2 f = 0$$

with the solution

$$f(r) = -\alpha\kappa H_1(\kappa r) - \beta\kappa J_1(\kappa r) ,$$

where $H_1(x)$ and $J_1(x)$ are first order Hankel and Bessel functions, and α and β are arbitrary constants.

Further solution of (7) leads to the following expression for $A(r)$

$$A(r) = -\gamma r/2 + \delta/r - \alpha H_1(\kappa r)/\kappa - \beta J_1(\kappa r)/\kappa ,$$

where γ and δ is another pair of constants. Now from equations (6) and (8) general solution for the velocity components and pressure can be found

$$u_r = \left(v - \frac{\gamma}{2} + \frac{\delta}{r^2} - \alpha\frac{H_1(\kappa r)}{\kappa r} - \beta\frac{J_1(\kappa r)}{\kappa r}\right)\cos\theta ,$$

$$u_\theta = -\left(v - \frac{\gamma}{2} - \frac{\delta}{r^2} - \alpha\left(H_0(\kappa r) - \frac{H_1(\kappa r)}{\kappa r}\right) - \beta\left(J_0(\kappa r) - \frac{J_1(\kappa r)}{\kappa r}\right)\right)\sin\theta ,$$

$$p = -\frac{\eta}{a^2}\kappa^2\left(\frac{\gamma}{2} + \frac{\delta}{r^2}\right)ra\cos\theta .$$

Constants α, β, γ and δ are determined from the boundary conditions (2)-(5) as

$$\alpha = \frac{2v(1-\phi)}{Z_0(2-\phi) - Z_1\left(2(1-\phi) - (2-\phi)\dfrac{Kn\kappa^2}{(1+2Kn)}\right)} ,$$

$$\beta = -\alpha H_1(\kappa / \sqrt{1-\phi})/J_1(\kappa / \sqrt{1-\phi}) ,$$

$$\gamma = v \frac{2(1-\phi)\left(Z_0 - Z_1\left(2 - \frac{Kn\,\kappa^2}{(1+2Kn)}\right)\right)}{Z_0(2-\phi) - Z_1\left(2(1-\phi) - (2-\phi)\frac{Kn\,\kappa^2}{(1+2Kn)}\right)},$$

$$\delta = -\gamma/(2(1-\phi)),$$

where

$$Z_0 = H_0(\kappa) - H_1(\kappa/\sqrt{1-\phi})J_0(\kappa)/J_1(\kappa/\sqrt{1-\phi}),$$

$$Z_1 = \frac{1}{\kappa}\left(H_1(\kappa) - H_1(\kappa/\sqrt{1-\phi})J_1(\kappa)/J_1(\kappa/\sqrt{1-\phi})\right)$$

Complex tortuosity is defined as the ratio of the macroscopic pressure gradient $-\partial_x P$ in the direction of the sound propagation to the resulting averaged force per unit volume of the fluid $\langle F_x \rangle = -i\omega\rho_0\langle v_x \rangle$:

$$\alpha(\omega) = \partial_x P/(i\omega\rho_0\langle u_x \rangle)$$

As all the fluid is contained within the cells the velocity averaging is performed over the cell volume [9]:

$$\langle u_x \rangle = \int_0^{2\pi}\int_1^{r_{out}} u_x(r,\theta)r\,dr\,d\theta / S_{cell},$$

where $u_x = u_r \cos\theta - u_\theta \sin\theta$ and $S_{cell} = \pi\phi/(1-\phi)$ is the normalized cross sectional area of the cell. The final expression for the complex tortuosity, i.e.

$$\alpha_\perp(\omega,K) = \left((2-\phi) - \frac{4(1-\phi)Z_1}{\phi\left(Z_0 + Z_1\left(\frac{2(1-\phi)}{\phi} + \frac{Kn\,\kappa^2}{1+2Kn}\right)\right)}\right),\quad (10)$$

depends amongst other parameters on the Knudsen number Kn. In this equation subscript $\perp$ indicates sound propagating perpendicular to cylinder axes.

If the oscillatory pressure gradient direction is parallel to fibre axis z, incompressible fluid has just one velocity component along this axis, which varies with the distance r from the fibre centre and independent on the angle θ. Equations of motion (1) in this case should be replaced by one simpler equation:

$$-i\omega\rho_0 u_z = \eta(\partial_{rr} u_z + \partial_r u_z/r)/a^2 - \partial_z P, \quad (11)$$

Its general solution is

$$u_z(r) = \partial_z P/(i\omega\rho_0) + \alpha_1 J_0(\kappa r) + \beta_1 H_0(\kappa r)$$

Coefficients α_1 and β_1 can be found from Knudsen boindary condition on the fibre surface

$$u_z(r=1) = Kn\partial_r u_z(r=1) \quad (12)$$

(the fact that $\tau_{r\theta} = \eta\partial_r u_z$ was used here)

and boundary condition of zero vorticity on the outer cell surface

$$\partial_r u_z(r = 1/\sqrt{1-\phi}) = 0 \quad (13)$$

as $\alpha_1 = \dfrac{H_1(\kappa/\sqrt{1-\phi})}{J_1(\kappa/\sqrt{1-\phi})}\dfrac{\partial_z P/(i\omega\rho_0)}{Z_0 + Kn\,\kappa^2 Z_1}$ and

$$\beta_1 = -\frac{\partial_z P/(i\omega\rho_0)}{Z_0 + Kn\kappa^2 Z_1}$$

Particle velocity averaged over the cell volume $\langle u_z \rangle$ in this case can be reduced to the following integral

$$\langle u_z \rangle = 2\pi\int_1^{r_{out}} ru_z\,dr/S_{cell} = \frac{\partial_z P}{i\omega\rho_0}\left(1 + \frac{2(1-\phi)Z_1}{\phi(Z_0 + Kn\,\kappa^2 Z_1)}\right)$$

Finally, following the equation for the complex tortuosity the following expression is obtained

$$\alpha_{||}(\omega,Kn) = \left(1 - \frac{1}{\phi}\frac{2(1-\phi)Z_1}{Z_0 + Z_1\left(2\frac{1-\phi}{\phi} + Kn\,\kappa^2\right)}\right),\,(14)$$

where subscript $||$ indicates sound propagating parallel to cylinder axes.

2.2 Complex compressibility

Now let's consider the heat transfer between a cylindrical fibre subject to oscillating pressure $Pe^{-i\omega t}$ and the surrounding fluid. The amplitude of the temperature distribution T in the fluid does not vary with the sound propagation direction and can be found from the equation of heat transfer [2]:

$$N_{pr}\kappa^2 T - (\partial_{rr}T + \partial_r T/r) = (N_{pr}\kappa)^2 P/(\rho_0 c_p)\,(15)$$

presented here in cylindrical coordinates. Here N_{pr} is the Prandtl number. The boundary condition on the fibre surface accounting for the thermal slip is:

$$T(1) = 2\gamma Kn\partial_r T/((\gamma+1)N_{pr}), \quad (16)$$

where γ is adiabatic constant, and the zero temperature gradient is assumed on the outer cell boundary [10]

$$\partial_r T(1/\sqrt{1-\phi}) = 0. \quad (17)$$

Comparison of equations (15)-(17) with (11)-(13), suggests that

$$T(\omega,Kn) = \frac{-N_{pr}\kappa^2 P/(\rho_0 c_p)}{a^2\partial_z P/\eta}u_z\left(\omega N_{pr}, \frac{2\gamma Kn}{N_{pr}(\gamma+1)}\right)$$

Using this relationship and the following definition of the normalised complex compressibility function

$$C(\omega,Kn) = \gamma(1 - \rho_0 R_{gas}\langle T(\omega,Kn)\rangle/P)$$

where R_{gas} is a specific gas constant, the relationship between complex compressibility of the cylinder array and its complex tortuosity f $\alpha_{||}$ can be easily derived:

$$C(\omega,Kn) = \left(\gamma - (\gamma-1)/\alpha_{||}\left(\omega N_{pr}, \frac{2\gamma Kn}{N_{pr}(\gamma+1)}\right)\right),\,(18)$$

3 Model predictions and comparisons with FEM results

Complex density and complex compressibility functions obtained in the previous section can be used for calculation of the characteristic impedance and the propagation of the array using the following equations

$$Z_{||,\perp}(\omega, Kn) = \frac{\rho_0 c}{\phi} \sqrt{\alpha_{||,\perp}(\omega, Kn)/C(\omega, Kn)},$$

$$k_{||,\perp}(\omega, Kn) = \frac{\omega}{c} \sqrt{\alpha_{||,\perp}(\omega, Kn)C(\omega, Kn)}, \qquad (19)$$

and hence fully determining its acoustical properties. Here the influence of the boundary slip on sound speed $c_{||,\perp}(\omega, Kn) = \omega/\mathrm{Re}(k_{||,\perp}(\omega, Kn))$ and attenuation coefficient $\alpha_{||,\perp}(\omega, Kn) = \mathrm{Im}(k_{||,\perp}(\omega, Kn))$ will be investigated and compared with the results of numerical computations. The latter have been obtained using the FEM software Comsol Multiphysics. Second-order Lagrangian elements have been used to model the velocity components and temperature distribution, whereas the linear elements approximated the pressure field. An oscillatory forced Stokes flow problem has been solved assuming that the total force vanishes and the periodic boundary conditions are applied on the boundary of the square cell. The latter has been imposed to allow for interactions between the circular cylinders. An arbitrary reference pressure was prescribed in one of the vertices of the square cell. Knudsen boundary condition was applied at the cylinder surface. The macroscopic velocity was obtained from the solution of the perpendicular/parallel oscillatory forced Stokes flow problem by averaging over the cell and complex tortuosity has been then calculated from its definition. The oscillatory heat conduction problem has been solved in a unitary square cell assuming thermal slip on the cylinder surface and periodicity conditions on the cell boundary. The cell averaged temperature was then estimated from the solution of the above problem and the dynamic compressibility was calculated. Using complex tortuosity and complex compressibility functions, the speed of sound and attenuation coefficient has been found.
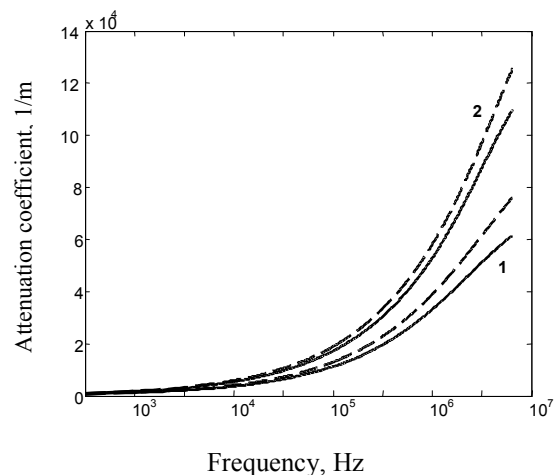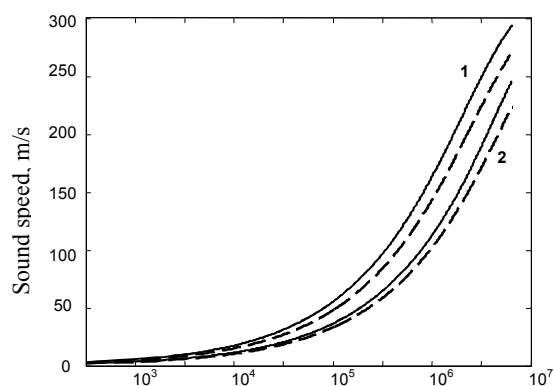
Figure 2. Sound speed and attenuation coefficient, analytical model for sound parallel (1) and perpendicular (2) to cylinder axes. Cylinder radius 200 nm, porosity 0.95. Dashed line – no-slip, solid line – *Kn*=0.3.

Predictions of the analytical model, shown in Figure 2, confirm, that the correct account of the boundary slip leads to higher sound speed and lower attenuation coefficient values compared to no-slip case. To quantify the slip influence the relative increase of the sound speed $\Delta_c = |c(\omega, Kn) - c(\omega, 0)|/c(\omega, 0)$ and relative decrease of the attenuation coefficient $\Delta_\alpha = |\alpha(\omega, Kn) - \alpha(\omega, 0)|/\alpha(\omega, 0)$ have been calculated for several values of the Knudsen number and are presented in Figure 3 assuming sound propagation parallel to cylinder axes. For the array of cylinders with a=120nm for instance, both sound speed and attenuation coefficient calculated assuming no-slip boundary conditions differ by more than 20% from values obtained with corrected boundary conditions in the whole range of frequencies. The error, naturally, decreases as the cylinder radius increases. Relative errors obtained for the array of fibres with axes perpendicular to sound propagation direction are lower than those shown in Fig.3, which means that the effect of boundary slip is weaker in this case. However, those values are still considerable, reaching 12% for a=120nm. Comparisons between numerical and analytical results show excellent agreement for high porosity arrays. However, for relatively dense arrays analytical model becomes inaccurate. The relative error between the analytical and numerical results for the sound speed assuming propagation parallel to fibre axes is shown in Figure 4.
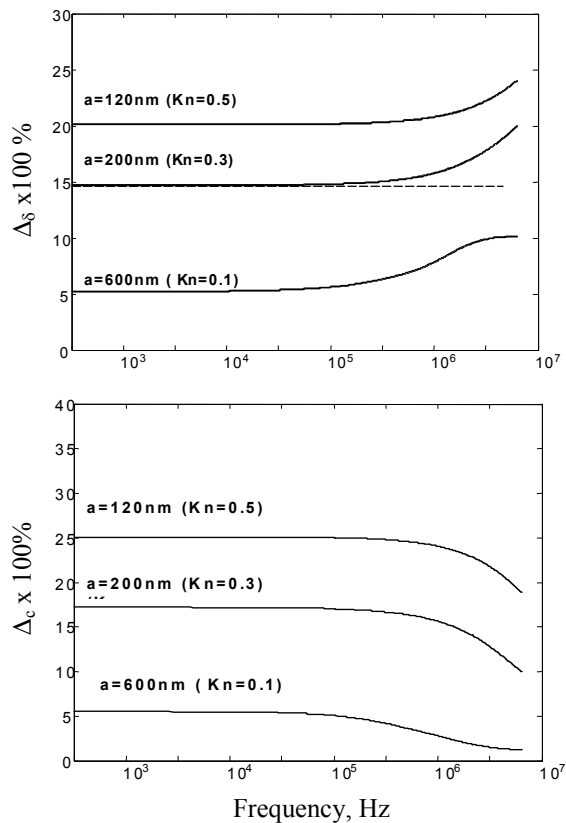
Figure 3. Relative influence of boundary slip

on attenuation coefficient and sound speed at different fibre radii as a function of frequency, porosity 0.95, fibres parallel to sound propagation direction. Analytical model.
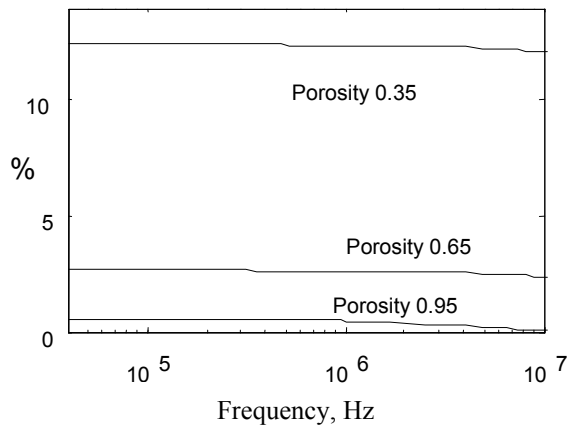
Figure 4. Relative error of the analytical model compared to FEM simulations, sound speed, *Kn*=0.3

4   Conclusion

A simple analytical model, presented in this paper, confirms that the influence of the boundary slip on the acoustical properties of microfibrous absorbents can be very significant. Moreover, it is demonstrated, that this influence depends on the material geometry, not just on the size of the inclusions. For the array of cylindrical fibres effect of the boundary slip is more noticeable when sound propagates parallel to the fibre axes. In this case, even for the array of fibres as with radius as big as 200 nm the new model predictions of sound speed and attenuation coefficient vary by more than 15% compared to no-slip case. The analytical model is shown to be in a good agreement with numerical results when the array porosity is high. This leads to the conclusion that it can provide a basis for modelling the acoustical properties of real microfibrous materials, such as aerogels. It can also serve as a reasonable approximation for materials similar to activated carbon, which is impossible to model as a network of cylindrical pores due to its high porosity.

References

[1] D.A.Lockerby et al "Velocity boundary conditions at solid walls in rarefied gas calculations", Phys.Rev. E70, 017303 (2004)

[2] V.F.Kozlov, A.V.Fedorov, N.D.Malmuth "Acoustical properties of rarefied gases inside pores of simple geometries", J.Acoust.Soc.Am. 117, 3402-3411 (2005)

[3] N.G.Hadjiconstantinou, O.Simek "Sound propagation at small scales under continuum and non-continuum transport", J.Fluid.Mech., 488, 399 (2003)

[4] E.Skjetne, J.-L.Auriault "Homogenization of wall-slip gass flow through porous media", Transport in Porous Media, 36, 293-306 (1999)

[5] J.Chastanet, P.Royer, J.-L.Auriault "Acoustics with wall-slip flow of gas saturated porous media", Mechanics Research Communications 31, 277-286 (2004)

[6] D.Tsiklauri "Phenomenological model of propagation of the elastic waves in a fluid saturated porous solid with nonzero boundary slip velocity", J.Acoust.Soc.Am., 112, 843-849 (2002)

[7] M.G.Markov "Effect of the interfacial slip on the kinematic and dynamic parameters of elastic waves in a fluid –saturated porous medium", Acoust.Phys. , 53, 213-216 (2007)

[8] J.Gross, J.Fricke, L.W.Hrubesh "Sound propagation in SiO_2 aerogels", J.Acoust.Soc.Am. 91, 2004-2006 (1992)

[9] V.Tarnow "Calculation of the dynamic air flow resistivity of fiber materials", J.Acoust.Soc.Am., 102, 1680-1688 (1997)

[10] V.Tarnow "Compressibility of air in fibrous materials", J.Acoust.Soc.Am., 99, 3010-3017 (1996)